Volume 336, number 3, 375–380 FEBS 13418 December 1993

Molecular cloning, functional expression and localization of an inward rectifier potassium channel in the mouse brain

Ken-Ichirou Morishige[a], Naohiko Takahashi[a], Ian Findlay[c], Hidekazu Koyama[a], Jill S. Zanelli[a], Christine Peterson[d], Nancy A. Jenkins[e], Neal G. Copeland[e], Nozomu Mori[d], Yoshihisa Kurachi[a,b,*]

[a]*Division of Cardiovascular Diseases, Department of Internal Medicine, Mayo Clinic, Rochester, MN 55905, USA*
[b]*Department of Pharmacology, Mayo Clinic, Rochester, MN 55905, USA*
[c]*Universite de Tour, Tour, France*
[d]*Ethel Percy Andrus Gerontology Center, University of Southern California, Los Angeles, CA 90089, USA*
[e]*Mammalian Genetics Laboratory, ABL-Basic Research Program, NCI-Frederick Cancer Research and Development Center, Frederick, MD 21702-1201, USA*

Received 26 October 1993

We have cloned an inward-rectifier potassium channel from a mouse brain cDNA library, studied its distribution in the brain by in situ hybridization and determined the chromosomal localization of the gene. A mouse brain cDNA library was screened using a fragment of the mouse macrophage IRK1 cDNA as a probe. Two duplicate clones of ~5.5 kb were obtained. *Xenopus* ococytes injected with cRNA derived from the clone expressed a potassium channel with inwardly rectifying channel characteristics. The amino acid sequence of the clone was identical to that of IRK1 recently cloned from a mouse macrophage cell line. In situ hybridization study showed the mouse brain IRK1 to be generally distributed throughout the brain, but in particular subsets of neurons at high levels. The gene was placed in the distal region of mouse chromosome 11, which contains several uncloned neurological mutations. These results provide the first demonstration of the cloning and distribution of an inward rectifier potassium channel from the nervous system.

Inward rectifier potassium channel; cDNA library; Mouse brain; *Xenopus* oocyte; Hybridization, in situ; Chromosome mapping

1. INTRODUCTION

Inwardly rectifying potassium channels play a significant role in the maintenance of the resting membrane potential, in regulating the duration of the action potential and in controlling excitability of a variety of cell types including central nervous system cells [1–4].

An inward rectifier potassium channel (IRK1) has been recently cloned from a mouse macrophage cell line [5] which shows considerable homology with an ATP-dependent potassium channel cloned from rat kidney (ROMK1) [6]. Both of these channels show significant differences from classical voltage-gated potassium channels [7], since they show only two transmembrane segments with one pore-forming region. Northern blotting analysis has shown IRK1 mRNA to be expressed in various tissues including forebrain, cerebellum, heart and skeletal muscle, besides macrophage cell line [5]. The Northern analysis, however, did not rule out the possibility that the brain may express an IRK1 related sequence(s) and also did not clarify whether IRK1 (or its related) mRNA is expressed in neurons or non-neuronal cells such as glia.

We have cloned, electrophysiologically characterized, and localized an inward rectifier potassium channel from the mouse brain, and determined the location of the gene on mouse chromosomes. This is the first demonstration of the cloning and distribution of an inward rectifier potassium channel from the central nervous system.

2. MATERIALS AND METHODS

2.1. *Screening of mouse brain cDNA library and DNA sequencing*

A mouse brain cDNA library (Stratagene, La Jolla, CA) was screened under a mild stringency condition using a *Bst*XI–*Not*I digested IRK1 (~3.8 kb) as a probe. IRK1 was kindly provided by Dr. Lilly Y. Jan (UCSF, San Francisco, CA) [5]. 2×10^5 Phage clones were screened with a ^{32}P-labelled probe. Hybridization was done at moderate stringency as described [8], filters were washed with 0.1 × SSC, 0.5% sodium deoxy sulfate (SDS) at room temperature for 20 min, and then exposed to X-ray film overnight at −70°C with intensifying screen. DNA sequencing was performed on both strands using a sequencing kit (USB, Cleveland, OH) by specific oligonucleotide primers as previously described [8].

*Corresponding author. Department of Pharmacology, Mayo Foundation, Rochester, MN 55905, USA. Fax: (1) (507) 284 9111.

Abbreviations: IRK, inward rectifier potassium channel; cDNA complementary deoxyribonucleotic acid; cRNA, complementary ribonucleic acid; mRNA, messenger ribonucleic acid; SCC, saline-sodium citrate; SDS, sodium dodecyl sulfate; TH, tyrosine hydroxylase; GABA, γ-amino-*n*-butyric acid.

2.2. *Functional expression of a mouse brain inward rectifier potassium channel in* Xenopus *oocytes*

One of two positive clones thus obtained was transcribed in vitro by T_3 RNA polymerase after digestion with *Apa*I as described [8]. This transcript was dissolved in sterile water, and injected to manually defoliculated oocytes (50 nl of 100 ng/μl). After injection, oocytes were incubated in a modified Barth solution at 18°C, and electrophysiological studies were undertaken 48–96 h later after injection.

Two-electrode voltage clamp (Turbo Clamp TEC 01C, Tamm, Germany) experiments were performed with microelectrodes which, when filled with 3 M KCl, had resistances of 0.5–1.5 MΩ. Oocytes were bathed in a solution which contained 90 mM KCl, 3 mM $MgCl_2$, 5 mM HEPES (pH adjusted to 7.4 with KOH) and 150 μM niflumic acid to block endogenous chloride current. Oocytes were voltage-clamped at 0 mV and voltage-steps of 1.5 s duration were applied to the cells from −160 to +60 mV in 10 mV increments every 5 s. Single channel recordings were made in the cell-attached patch configuration using a patch clamp amplifier (Axopatch 200A, Axon Instruments, Foster City, CA). Both pipette and bath solutions contained 140 mM KCl, 1.4 mM $MgCl_2$ and 10 mM HEPES (pH adjusted to 7.4 with KOH). Experiments were performed at room temperature (20–22°C). Data from electrophysiological recordings were stored on video tape using a PCM data recording system and subsequently replayed for computer analysis.

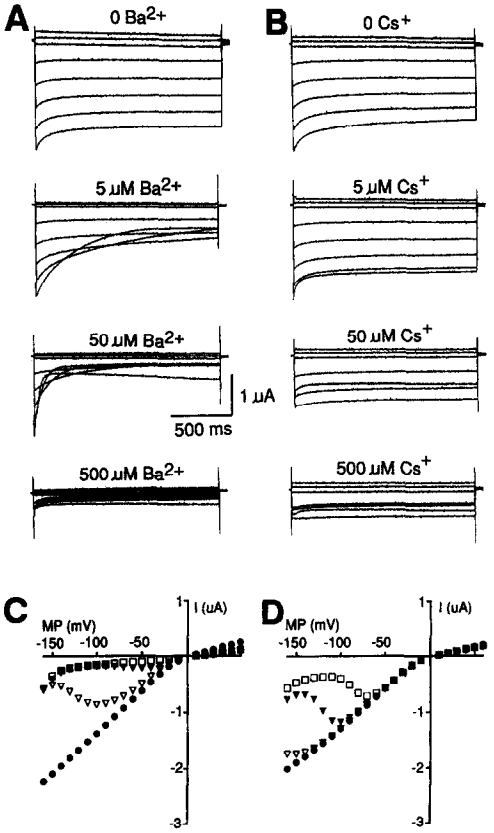

Fig. 1. Cell currents recorded from a *Xenopus* oocyte expressing the MB-IRK1 clone. A and C illustrate currents induced by voltage steps from 0 mV to, in descending order, +50, +20, −10, −40, −70, −100, −130 and −160 mV (the full sequence of voltage steps is not shown for clarify). The upper traces in each column show records obtained under control conditions. (A) The effect of external Ba^{2+}. The labels above each family of traces indicate the concentration of Ba^{2+} which had been included in the solution which bathed oocyte. (B) Current voltage relationships of the steady-state currents recorded from this oocyte in the presence of Ba^{2+}. (C) The effects of external Cs^+. Labels above each trace indicate the concentration of Cs^+ which had been included in the bathing solution. The time and cell current scales are applicable to all of these traces which were recorded from one oocyte. (D) Current–voltage relationships recorded in the presence of Cs^+. Circles, control; open triangles, 5 μM cation; filled triangles, 50 μM cation; squares, 500 μM cation.

2.3. *In situ hybridization*

In situ hybridization was carried out essentially as described previously [9,10]. Brains from 13-day-old and 12-month-old C57BL/6J mice (Charles River, Gilroy, CA) were frozen on powdered dry ice, and 15 μm coronal, parasagittal and horizontal sections were cut with a cryostat, thaw-mounted on gelatin-coated slides, and stored at −80°C until analyzed. The sections were postfixed, acetylated, dehydrated, and then hybridized in situ with ^{35}S-labeled sense or antisense IRK1 cRNA probe. A 2 kb insert containing the coding region (the 5′ most *Eco*RI–*Nhe*I fragment) was subcloned into pBluescriptII SK- (Stratagene). This plasmid, pMB2, was linearized with *Stu*I or *Bam*HI, and RNA was synthesized in vitro in the presence of [α-^{35}S]UTP (DuPont/NEN, Boston, MA) using T3 or T7 polymerase for sense and antisense probes, respectively. An antisense probe corresponding to the 3′-non-coding region was also generated on the *Not*I-linearized MB11 template. Hybridization was performed at 50°C for 12–16 h, and sections were treated with RNase then washed under high stringency conditions. Dehydrated sections were exposed to Fuji RX film for 2–3 days. For higher resolution, the slides were dipped in diluted Kodak NTB-2 nuclear emulsion and exposed at −20°C for 8–12 days. After development, sections were counter-stained with Cresyl violet. Photographs were taken using the X-ray film as a negative. Bright-field and dark-field images of emulsion dipped slides were taken using a microscope.

2.4. *Mouse chromosome mapping*

Chromosome mapping of the *Irk1* gene was performed as previously described by interspecific mouse backcross analysis [12]. This interspecific backcross mapping panel has been typed for over 1,400 loci that are well distributed among all the autosomes as well as the X chromosome [13]. The probe that was used for mapping was a ca. 350 bp DNA fragment containing the 316 bp region that corresponds to amino acid residues 74–179 [5]. A description of the probes and restriction fragment length polymorphisms (RFLPs) for most loci linked to the mouse *Irk1* gene has been reported previously [11]. Recombination distances were calculated, and gene order was determined by minimizing the number of recombination events required to explain the allele distribution patterns.

3. RESULTS

3.1. *Molecular cloning of inward rectifier potassium channel*

After screening of 2×10^5 mouse brain cDNA clones, we obtained two positive clones. These phage inserts were subcloned into plasmids by rescue excision to generate MB6 and MB11. The insert size of these two clones were ~5.5 kb. The analysis of the insert size and the restriction map indicated that these two clones were duplicate each other. Accordingly, we used MB11 as a template for preparing cRNA and for DNA sequencing. The deduced 428 amino acid sequence of the MB11 was exactly identical to that of IRK1 that has recently been cloned from a macrophage cell line [5] except for some nucleotide differences in the 5′ non-coding region. Thus, we call this clone as MB-IRK1.

3.2. *Electrophysiological characteristics of MB-IRK1 current*

Fig. 1 illustrates the results obtained from one

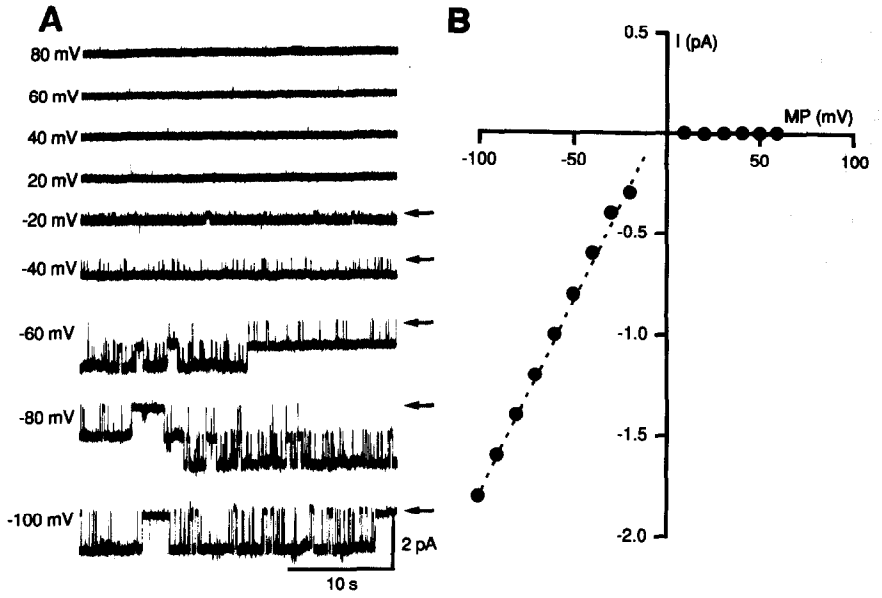

Fig. 2. Single channel recordings from a cell-attached membrane patch of a *Xenopus* oocyte expressing the MB-IRK1. (A) Membrane current traces recorded at the membrane potential values indicated to the left of each trace. The time and current scales are applicable to each of these traces. The arrows to the right of certain traces indicate the patch current level recorded when all channels were closed. This patch appeared to contain only two MB-IRK1 inwardly rectified potassium channels. (B) The current–voltage relationships of the channel record shown in (A). The cut off frequency was 1 kHz.

Xenopus oocyte which had been injected with cRNA derived from MB-IRK1 48 h before the recording. Under control conditions (top traces in Fig. 1A,C), voltage steps from a holding potential of 0 mV revealed a large current with clear inwardly rectifying properties which showed slight voltage-dependent inactivation at extreme hyperpolarizing voltages. The current–voltage relationship for the steady-state current recorded 1.5 s after the onset of the voltage step (Fig. 1B,D) was linear for inward currents at negative potentials with a slope conductance of 16.0 ± 3.5 μS (mean ± S.D., $n = 4$). Outward membrane currents at positive potentials were considerably less than that predicted by a linear current–voltage relationship. External Ba^{2+} (Fig. 1A,B) concentration-dependently induced a time- and voltage-dependent block of the inward currents expressed by

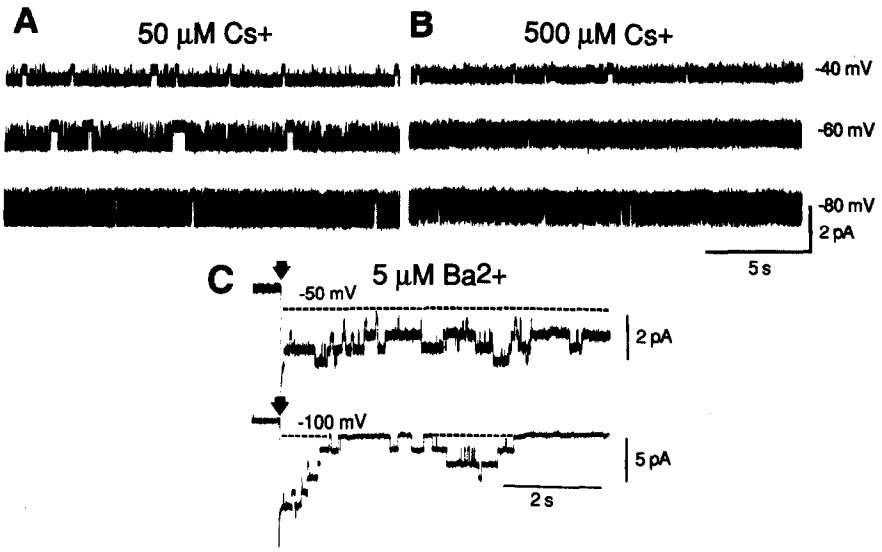

Fig. 3. Cs^+ or Ba^{2+} block of the MB-IRK1 inward rectifier potassium channel. These records were all obtained from cell-attached membrane patches. (A and B) The effects of external Cs^+ are shown in two groups of records obtained from different oocytes at the membrane potentials indicated with each trace. Downward deflections of the current record represent inwardly directed membrane currents. (C) The effects of Ba^{2+} are shown in two traces where the membrane voltage was switched from 0 mV to ~50 mV (upper trace) or to ~100 mV (lower trace) at the times indicated by the arrows above the traces. The capacitance and resistance of the seal between the pipette and the oocytes have not been compensated. The dotted lines represent the patch current level recorded when all channels were closed during voltage steps.

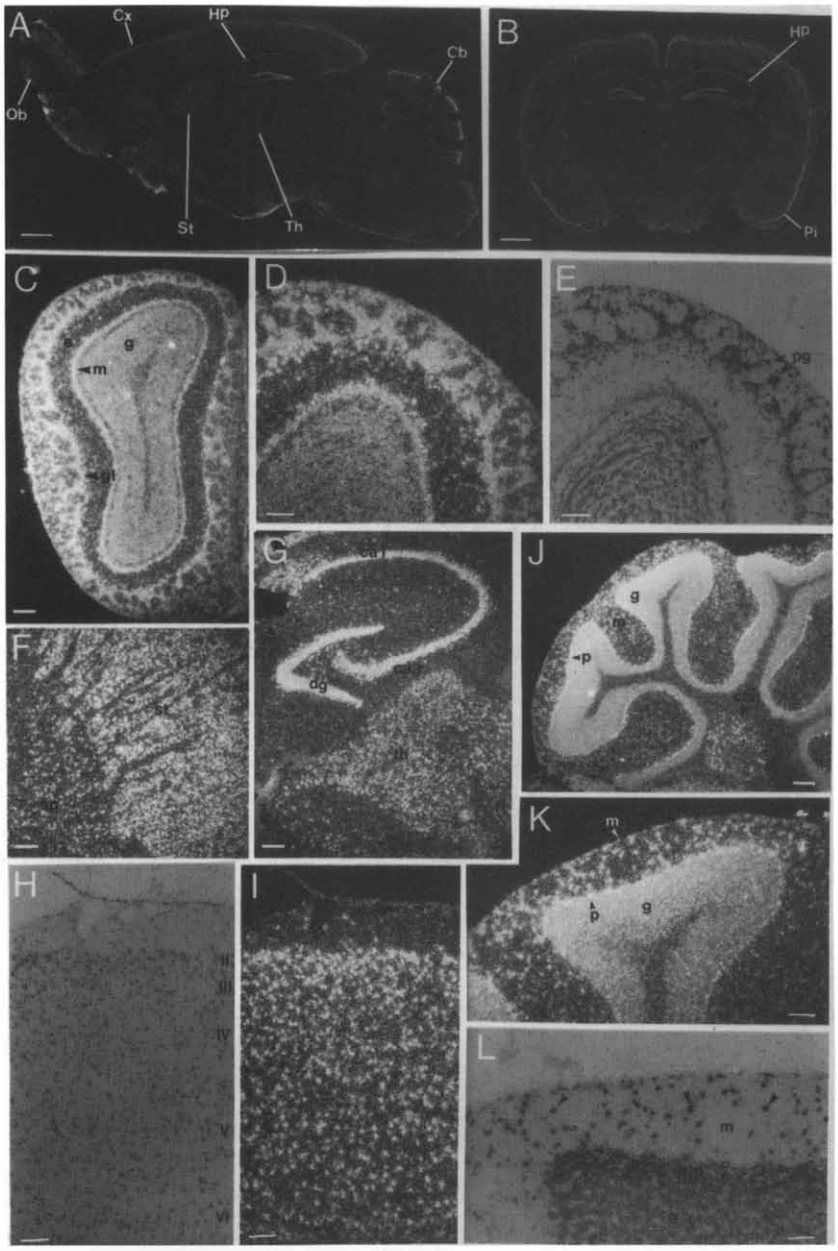

Fig. 4. MB-IRK1 mRNA localization in adult mouse brain (A and B). In situ hybridization images of parasagittal and coronal sections that were reproduced from X-ray film. Cb, cerebellum; Cx, cortex; Hp, hippocampus; Ob, olfactory bulb; Pi, piriform cortex; St, striatum; Th, thalamus. Scale bar = 1 mm (C–E). Low-power magnification of emulsion-dipped slide of the olfactory bulb: g, internal granule cell layer; m, mitral cell layer; e, external plexiform layer; gl, glomerular layer. Note the intense labelling of periglomerular (pg) cells around the glomerular cells. C and D: dark-field. E: bright-field. Scale bars; 200 μm in C; 100 μm in D and E. (F) Dark-field photomicrograph of the striatal (st) and septal (sp) regions in a parasagittal section. Scale bar = 200 μm. (G) Dark-field photomicrograph of the thalamus (th) and hippocampus: dg, dentate gyrus = granule cell layer; ca1 and ca3 = pyramidal cell layer. Scale bar = 200 μm. (H and I) Bright-field and dark-field photomicrographs of the frontal cortex. Laminar structure (layers II through VI) are indicated based upon the Nissl stained sections. Scale bars = 100 μm. (J–L) Low and high magnifications views of the cerebellum layers showing high expression of MB-IRK1 mRNA in cells of the molecular layer (m): g, granule cell layer; p, Purkinje cell layer. J and K, dark-field; L, bright-field. Scale bars for J, K, and L = 200, 100, and 50 μm, respectively.

MB-IRK1. 5 and 50 μM Ba^{2+} clearly illustrate this time- and voltage-dependence with comparatively little effect upon the instantaneous current (Fig. 1A) but a marked influence upon the steady-state current (Fig. 1B). 500 μM Ba^{2+} essentially abolished the oocyte inward current, both instantaneous and steady-state. The blocking effect of Cs^+ on the MB-IRK1 currents was little time-dependent but clearly concentration and voltage-dependent (Fig. 1C,D). Even 500 μM Cs^+ was essentially without effect at potentials positive to −70 mV (Fig. 1D).

Single channel current records obtained from cell-

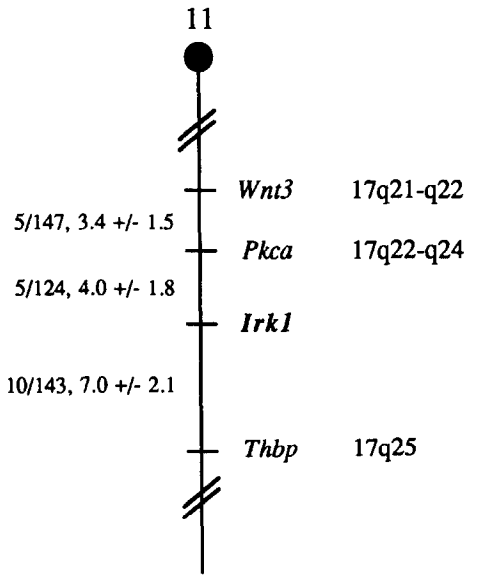

Fig. 5. *Irk1* maps in the distal region of mouse chromosome. 11. *Irk1* was placed on mouse chromosome 11 by interspecific backcross analysis. A partial chromosome 11 linkage map showing the location of *Irk1* in relation to linked genes is shown. The number of recombinant animals over the total number of animals typed for each pair of loci and the recombination distances between loci in centimorgans (± standard error) are shown to the left of the chromosome and the positions of loci in the human chromosomes, where known, are shown to the right. References for the map positions of most human loci can be obtained from GDB (Genome Database), a computerized database of human linkage information maintained by The Williams H. Welch Library of The Johns Hopkins University (Baltimore, MD).

attached membrane patches on oocytes which expressed the MB-IRK1 were shown in Fig. 2A. The currents passing through MB-IRK1 channels were observed in the inward direction and thus showed a strong inward-rectifying property (Fig. 2B). The unit conductance of the channel was 20.4 ± 0.9 pS (n = 4).

When 50 μM Cs^+ was included in the pipette solution (Fig. 3A), the open channel current record was interrupted by brief transitions from the conductive to a non-conductive condition. The frequency of these interruptions increased with hyperpolarization. With 500 μM Cs^+ in the pipette solution, interruptions became so frequent that the channel open current level was apparently reduced by the low bandwidth on the recording. Thus, the transitions of channels between unblocked and blocked states with Cs^+ were very rapid, which is consistent with the instantaneous block of the whole cell current by Cs^+.

When the pipette solution contained Ba^{2+} (Fig. 3C), on the other hand, voltage steps to strong hyperpolarizing potentials clearly induced a slowly-developed time-dependent block of single MB-IRK1 channels as noticed in the two-electrode voltage clamp experiment (Fig. 1A,B). In the example shown in Fig. 3C, the membrane patch contained at least five channels. A voltage step from 0 mV to −50 mV revealed a channel record characterized by a series of openings and apparent closing of the MB11 channels. This pattern was maintained for the duration of the voltage step. But when the membrane voltage was stepped from 0 to −100 mV (lower trace of Fig. 3C), the record began with five simultaneously open channels which, within 1 s of the onset of the voltage step, had been blocked.

3.3. *Regional distribution of MB11 (IRK1) mRNA in the mouse brain*

The distribution of MB-IRK1 mRNA in mouse brain was analyzed by in situ hybridization. Specific cRNA probes revealed that the MB-IRK1 channel gene is widely expressed in the adult mouse brain (Fig. 4). MB-IRK1 antisense probes containing the coding region and 3′-noncoding region both showed identical profiles, while the sense probe did not show significant hybridization (data not shown). The overall distribution profile of MB-IRK1 mRNA in both parasagittal and coronal sections when compared to the neural specific marker SCG10 (not shown) suggested that MB-IRK1 is expressed in most of brain neurons, but probably not in glia (Fig. 4A,B). While MB-IRK1 mRNA was expressed in many neuronal structure throughout the brain, it was detected in certain neuronal populations at high levels. For example, in the olfactory bulb all neurons including inner granule cells, mitral cells and tufted cells were positive, but periglomerular cells that surround the glomeruli were intensely labelled (Fig. 4C–E). These periglomerular cells are also positive with tyrosine hydroxylase (TH) mRNA (not shown). Striatal neurons that are mostly GABAergic also showed moderate to high levels of expression (Fig. 3F). In the hippocampus both pyramidal cells in CA1 through CA3 regions and granule cells in dentate gyrus expressed MB-IRK1 mRNA, but the level of expression was higher in dentate granule cells (Fig. 4G, see also Fig. 4A,B). In the cerebral cortex MB-IRK1 mRNA expression was related to laminar structure. The MB-IRK1 probe labeled layer II neurons more than the larger pyramidal neurons in layer V (Fig. 4H,I). These MB-IRK1 signals in layer II become continuous with the piriform cortex (see Fig. 4B). In the cerebellum, MB-IRK1 mRNA was detected in granule cells and Purkinje cells, but interestingly the mRNA was also detected in cells in molecular layer (Fig. 4J–L). The MB-IRK1 strongly positive cells that are scattered in the cerebellar molecular layer may be stellate cells and/or basket cells (shown with arrowheads in Fig. 4L). These results indicate that MB-IRK1 is expressed in various central neurons but notably high levels in certain subset neurons.

3.4. *Localization of Irk1 gene on the mouse chromosome 11*

We used a short (0.35 kb) PCR clone as a probe for chromosome mapping by inter specific backcross. This probe detected single locus in mouse chromosomes and

no *Irk1* related sequences were found at high stringency conditions (data not shown). The *Irk1* locus mapped to the distal region of mouse chromosome 11 (Fig. 5). The *Irk1* gene located between previously assigned loci of *Pkca* and *Thbp* (see [13] for review). The distal region of mouse chromosome 11 shares a region of homology with human chromosome 17q (see [13] for review). In particular, *Pkca* has been positioned at 17q22-q24 and *Thbp* at 17q25. Our assignment of the mouse *Irk1* gene between the *Pkca* and *Thbp* loci suggests that the human *Irk1* gene will reside on human chromosome 17 probably between q22 and q25.

4. DISCUSSION

In the present study, we describe the amino acid sequence, the electrophysiological characteristics and the localization in the brain of an inward rectifier potassium channel cloned from mouse brain. We also identified the location of the gene on mouse chromosomes. This is the first description of a neuronal inward rectifier potassium channel at the molecular level. The amino acid sequence of MB-IRK1 shows 100% identity with that recently described for an inward rectifier potassium channel (IRK1) from a mouse macrophage cell line [5] except for slight differences in the non-coding 5′ region where MB-IRK1 lacks six nucleotides found in IRK1.

The electrophysiological characteristics of MB-IRK1 were classically the same as those of inward rectifier potassium channels found in a variety of cell types, such as absence of current at potentials positive to E_K, time- and voltage-dependent block by Ba^{2+} and Cs^+ [1–4]. At the level of single channel recording one characteristic worthy of note was the conductance, 20.4 pS, which is smaller than one normally associates with other inward rectifier potassium channels [3,4]. Further analysis of the MB-IRK1 channel, in excised membrane patches, for example, are required.

Northern blot analysis has shown the macrophage clone IRK1 to be prominently expressed in the central nervous system [5]. We have taken this analysis further by performing in situ hybridization studies using the MB-IRK1 cRNA as a probe. Although mRNA encoding the channel appeared to be fairly generally distributed in brain neurons, as one might expect since inward rectifier potassium channels are major regulators of neuronal excitability, significantly higher expression of MB-IRK1 mRNA occurred in granule cells in the periglomerular layer of olfactory bulb and the molecular layer of cerebellum, i.e. periglomerular cells and stellate cells, respectively. These cell populations interact with large pyramidal-type cells, i.e. mitral cells and Purkinje cells. Therefore, MB-IRK1 may contribute to modulate synaptic efficiency in these connections. The existence of MB-IRK1 and predicted structure of this channel will allow progress to be made in our understanding of the regulation of neuronal excitability at the molecular level.

Chromosomal mapping revealed that the MB-IRK1 gene (*Irk1*) locates in the distal region of mouse chromosome 11. This region of a mouse chromosome 11 contains a few uncloned neuronal mutations, such as *cod* (cerebellar outflow degeneration [14]) and *js* (Jackson shaker [15]). These observations may suggest the possible link of MB-IRK1 channel with these neurological disorder mutations.

Acknowledgements: This study was supported in part by grants from NIH RO1 HL 47360 (Y.K.), NIH AG07909 (N.M.) and the Max Factor Foundation (N.M.), and the National Cancer Institute, DHHS, under contract NOI-CO-74101 with ABL (N.A.J. and N.G.C.). This work has been performed during the tenure of the established investigatorship of the American Heart Association to Y.K. The authors thank Dr. Lilly Y. Jan (UCSF, San Francisco, CA) for the IRK-1 clone.

REFERENCES

[1] Inoue, M., Nakajima, S. and Nakajima, Y. (1988) J. Physiol. 407, 177–198.
[2] Fletcher, G.H. and Chiappinelli, V.A. (1992) Brain Res. 575, 103–112.
[3] Ishikawa, T., Wegman, E.A. and Cook, D.I. (1993) J. Membr. Biol. 131, 193–202.
[4] Kurachi, Y., (1985) J. Physiol. 366, 365–385.
[5] Kubo, Y., Baldwin, T.J., Jan, Y.N. and Jan, L.Y. (1993) Nature 362, 127–133.
[6] Ho, K., Nichols, C.G., Lederer, W.J., Lytton, J., Vassilev, P.M., Kanazirska, M.V. and Hebert, S.C. (1993) Nature 362, 31–38.
[7] Pong, O. (1992) Physiol. Rev. 72, 69–88.
[8] Sugimoto, T., Tsuchimochi, H., McGregor, C.G.A., Mutoh, H., Simizu, T. and Kurachi, Y. (1992) Biochem. Biophys. Res. Comm. 189, 617–624.
[9] Mori, N., Tajima, Y., Sakaguchi, H., Vandenbergh, D.J., Nawa, H. and Salvaterra, P.M. (1993) Mol. Brain. Res. 17, 101–111.
[10] Himi, T., Wang, H., McNeill, T.H. and Mori, N. (1993) Neuroscience, in press.
[11] Buchburg, A.M., Brownell, E., Nagata, S., Jenkins, N.A. and Copeland, N.G. (1989) Genetics 122, 153–161.
[12] Copeland, N.G. and Jenkins, N.A. (1991) Trends Genet. 7, 113–118.
[13] Copeland, N.G., Jenkins, N.A., Gilbert, D.J., Eppig, J.T., Maltais, L.J., Miller, J.C., Dietrich, W.F., Weaver, A., Lincoln, S.E., Steen, R.G., Stein, L.D., Nadeau, J.H. and Lander E.S. (1993) Science 262, 57–66.
[14] Sidman, R.L. (1980) Mouse News Lett. 63, 13.
[15] Dickie, M.M. and Deol, M.S. (1967) Mouse News Lett. 36, 39.